EFFECT OF A POROUS PARTITION ON THE FORMATION OF MOLECULAR FLOW

G. E. Gorelik, S. K. Zalenskii',
and N. V. Pavlyukevich

UDC 537.7:536.423.1

Numerical modeling is used to investigate how a curved evaporation surface and a highly porous partition over the mouth of a crucible affect the magnitude of molecular flow, its angular distribution, and the resulting condensate distribution on the base.

The thickness and uniformity of a coating, sputtered onto a rotating base in a vacuum chamber, depends on the source characteristics and on geometric parameters, which determine the relative dynamic position of the base and the mass source [1, 2]. A cylindrical or conical crucible, filled with the material to be sputtered, is often used as the mass source. The material, which is evaporated from the crucible by resistance, laser, or electron-beam heating, condenses on the base. The case of free molecular mass flow from a cylindrical or conical crucible, which is placed vertically or at an angle (in the case of a flat evaporation surface), has been examined in several publications [2, 3]. Here we examine how a highly porous partition over the mouth of the crucible affects the characteristics of the output molecular flow and on the resultant uniformity of the condensate on the surface of the base.

The problem is set up and solved within the framework of the mean-freepath approximation. It is assumed that the vapor pressure of the evaporated material in the channel (from the bottom of the crucible to its mouth) is such that the mean free path of the evaporated molecules is much larger than both the diameter of the channel and the mean free path inside the highly porous partition.

There are two standard approaches to examining this type of problem [4]. The first is usually used for simple geometries; it is related to deriving integral equations and solving them with approximate analytic or numerical techniques. The second approach – the Monte Carlo method – is not limited by the complexity of the partition; it models the physical process directly.

Here the Monte Carlo method is used to calculate the trajectories of sample particles which are evaporated from the spherical bottom of the channel. It is assumed that the flow of evaporating molecules is distributed uniformly over the bottom of the channel and that the angular distribution of the molecules follows a cosine law. Molecules are assumed to be absorbed when they strike the wall of the channel; then a fraction ε_w are absorbed by the wall and the fraction $(1 - \varepsilon_w)$ are diffusively reflected. For comparison, the calculation is repeated for elastic molecular reflection from the wall by the mirror law. The highly porous partition is modeled by selecting identical spheres of radius ρ, which are distributed uniformly throughout the volume of the partition (the "dusty gas" model [5, 6]). The flight path of the molecule λ in this model of the porous partition is calculated from an exponential law

$$f(\lambda) = (1/\lambda) \exp(-\lambda/\lambda_p),$$

where $f(\lambda)$ is the distribution of flight paths, and $\lambda_p = \frac{4}{3}\frac{p}{1-p}\rho$ is the mean free path of the molecule in the porous partition.

The sticking coefficient of the molecule on the surface of the spheres is taken as given ($0 \leq \varepsilon_s \leq 1$).

A. V. Lykov Institute of Heat and Mass Transfer, Academy of Sciences of the Belorussian SSR, Minsk. Translated from Inzhenerno-fizicheskii Zhurnal, Vol. 61, No. 4, pp. 621-625, October, 1991. Original article submitted June 20, 1990.

 0022-0841/91/6104-1254$12.50

TABLE 1. Basic Characteristics of the Molecular Flow

№	L	r_b	ε_w	δ_p	P	E	T	σ_t
			Dependence on the length of the mouth of the crucible					
1	0	∞	0	0	1	0	0,38	0,15
2	1	∞	0	0	0,67	0,33	0,27	0,15
3	2	∞	0	0	0,52	0,48	0,22	0,13
4	4	∞	0	0	0,36	0,64	0,15	0,11
			On the radius of curvature					
5	1	—1	0	0	0,42	0,58	0,16	0,16
6	1	—2	0	0	0,64	0,36	0,26	0,14
7	1	2	0	0	0,64	0,36	0,25	0,13
8	1	1	0	0	0,34	0,66	0,14	0,14
			On absorption on the walls					
9	1	∞	0,1	0	0,63	0,28	0,25	0,14
10	1	∞	0,5	0	0,49	0,13	0,21	0,11
11	1	∞	1,0	0	0,38	0	0,17	0,10
			On the thickness of the porous partition					
12	1	∞	0	0,2	0,44	0,55	0,18	0,17
13	1	∞	0	0,5	0,28	0,69	0,13	0,16
14	1	∞	0	1	0,16	0,77	0,07	0,14
15	2	∞	0	0,25	0,34	0,65	0,14	0,16
16	2	∞	0	0,50	0,25	0,72	0,11	0,18
17	2	∞	0	1	0,15	0,79	0,06	0,20

Note. A minus sign on r_b means a convex meniscus; a plus sign means a concave meniscus.

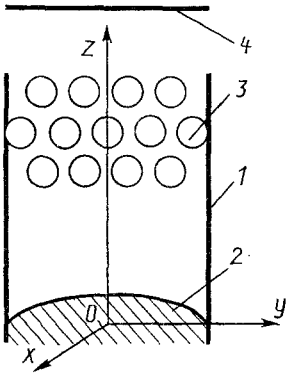

Fig. 1

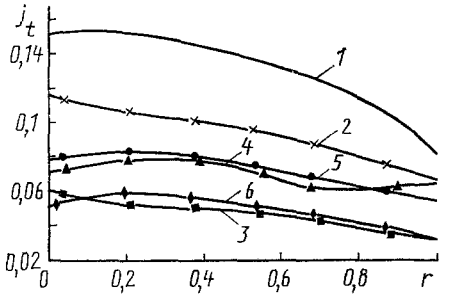

Fig. 2

Fig. 1. Diagram of the model: 1) crucible; 2) sputter material; 3) porous partition; 4) base.

Fig. 2. Molecular flow distribution over the surface of the base: 1) evaporation from surface; 2) free channel of length L = 1 with a flat meniscus; 3) the same with a spherical meniscus of radius $r_b = 1$; 4) channel with flat meniscus including absorption on the walls for $\varepsilon_w = 0.5$, L = 1, $r_b = \infty$; 5) free channel of length L = 2 with a flat meniscus; 6) channel with porous partition of thickness $\delta_p = 0.25$ for L = 2, $r_b = \infty$, $\varepsilon_w = 0$.

The modeling process starts by dividing the entire flow of the molecules from the bottom into N parts (the selection volume) from each of which sample particles are selected. Geometric parameters are introduced to model the porous partition: L, r_c, r_b, r_s, t_s, δ_p, p, and ρ. Interaction laws are specified for the sample molecules with the mouth of the channel and with the model spheres. The initial positions of the sample particles on the evaporation surface are chosen uniformly from the relationships:

$$z_0 = (r_b - \delta_z)\sqrt{(N - 0.5)/N}, \quad r_0 = \sqrt{r_b^2 - (\delta z + |z|)^2},$$
$$x_0 = r_0 \cos \varphi_0, \quad y_0 = r_0 \sin \varphi_0. \tag{1}$$

Here the plus sign refers to a convex meniscus and the minus sign to a concave one, and $\delta_z = \sqrt{r_b^2 - r_c^2}$.

In the case of axial symmetry ($x_0 = r_0$, $y_0 = 0$), the initial direction of the particles with respect to the normal at the point (x_0, y_0, z_0) is defined by the polar angle θ and the azimuthal angle ϕ, which are chosen randomly from the distribution $\theta = \arcsin\sqrt{R_\theta}$ and $\phi = 2\pi R_\phi$ and then transformed to the initial coordinate system using the formulas of spherical geometry. Then the flight path to collision with a model sphere of the porous partition is determined from $\lambda = -\lambda_p \ln R_\lambda$, to give the new position of the sample particle. Depending on the new position of the particle, a random choice is made for interaction with a sphere or with the corresponding boundaries. Particles which fall to the bottom of the channel or the base are assumed to be absorbed. Tracking the trajectories of the sample particles is terminated if the particle is absorbed or flows out of the channel and misses the target.

During the calculation, the position of absorbed particles and the direction of particle flying out of the channel are recorded to determine the volumetric distribution of particles that are absorbed in the porous partition, the distribution on bottom and walls of the channel, the distribution on the base, and the angular distribution of the particles which fly out of the channel.

The calculations showed that increasing the curvature of both a convex and concave evaporation surface, deepening the meniscus, increasing the sticking coefficients and the thickness of the porous partition all decrease the molecular flow from the channel. The flow onto the base is correspondingly reduced (see Table 1). As the length of the channel is increased, the effect of the curvature of meniscus does not decrease and remains significant (see Table 1).

It should be noted that when distances from the crucible to the base are comparable to the crucible dimensions, the uniformity of the coating is substantially affected by the spatial and local angular distributions over the area of the mouth of the crucible. Their total interaction is recorded by the flow distribution over the surface of a monitoring base (Fig. 1) located at one radius from the mouth of the crucible. As can be seen from Fig. 2, the uniformity of the coating varies rather weakly within the limits of the investigated parameter variations, in spite of the large flow variation. All linear dimensions in the figures are in a ratio to the radius of the channel.

If the distance from the crucible is large enough, so that the source dimensions can be neglected and the source can be considered to be a point source, the angular distribution of the molecules flying out of the channel play the basic role in the distribution of the coating over the surface of the base. Calculations showed that the angular distribution depends weakly on the curvature of the meniscus and on absorption inside the channel, and strongly on the channel length and the sticking coefficient of molecules to the wall (Fig. 3). As L and ε_w are increased, the distribution stretches out along the axis and the molecular flow becomes unidirectional. However, it is known that diffusion sources are preferred in industrial sputtering because they give sufficiently uniform coatings over large areas without additional equipment.

The possibility was investigated of smoothing the angular distribution with a highly

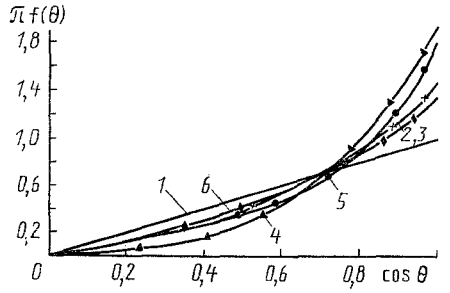

Fig. 3. Angular distribution of molecules flying out of the channel (the notation on the curves is the same as in Fig. 2; the values for the cases 2 and 3 are close and are shown as one curve in the figure).

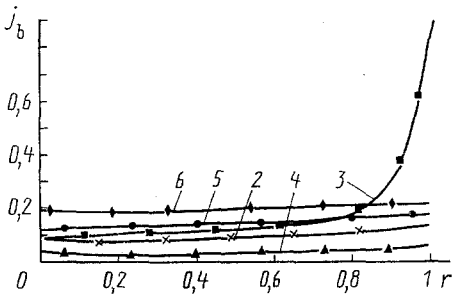

Fig. 4. Distribution of reverse flow at the bottom of the channel (curve notations are the same as in Fig. 2; for diffusion evaporation with a surface coating in the free molecular flow regime, there is no reverse flow, so curve 1 coincides with the abscissa).

porous partition, which would mix up the directions of the molecules and help homogenize the flow. The calculations showed that the angular distribution approached a diffusion distribution (Fig. 3) and the coating uniformity improved, if the partition thickness was on the order of one to a few mean free paths of the molecule in the porous medium. It should be noted that this improvement is accompanied by a decrease in the intensity of the outgoing flow.

The flow of molecules which return to the bottom of the crucible, as can be seen from Fig. 4, usually is less in the center of the bottom than at the edges; this tendency becomes stronger as the curvature of the meniscus is increased. Thus, if the material is sublimed from the solid phase, the nonuniformity of the reverse flow will make the central part of the sublimation front recess faster than the edges. This effect promotes formation of a concave meniscus, as a result of which the intensity of the outgoing flow can be reduced substantially.

NOTATION

p is the porosity; δ_p is the thickness of the porous layer; ρ is the radius of the model spheres for the porous layer; ε_s and ε_w are the sticking coefficients of molecules to the model spheres for the porous layer and to the walls of the channel, respectively; N is the number of sample particles; L is the channel depth; r_c, r_b, and r_s are the radii of the channel, the bottom of the crucible, and the base; t_s is the distance from the mouth of the channel to the base; θ and ϕ are the polar and azimuthal angles; x_0 and y_0 are the initial coordinates of the molecule; R_θ, R_ϕ, and R_λ are random numbers uniformly distributed in the interval [0, 1]; j_c and j_b are the current densities at the base and the bottom of the channel; $f(\theta)$ is the angular distribution density of the molecules flying out of the channel; $\sigma_t = \sigma(j_t)/j_t$ is the mean square deviation of the flow distribution along the base; P is transmission coefficient of the molecules; and E and T are the coefficients of absorption of molecules on the bottom of the crucible and the base.

LITERATURE CITED

1. I. A. Volchenok and G. E. Gorelik, "Mathematical modeling and optimum heat and mass transfer regimes for depositing multilayer coatings in a vacuum," Preprint Inst. Teplo. Mass. Akad. Nauk B.SSR, No. 46, Minsk (1987).
2. K. Nanbu, Vacuum, 36, No. 6, 349-354 (1986).
3. S. Stefanov, Material for the International Academic Seminar, Heat and Mass Transfer in Electronic and Microelectronic Systems Technology [in Russian], Minsk (1989), Chap. 2, pp. 61-67.
4. W. Stickelmacher, Rep. Prog. Phys., 49, 1083-1107 (1986).
5. B. V. Deryagin and S. P. Bakanov, Dokl. Akad. Nauk SSSR, 115, No. 2, 267-270 (1957).
6. N. V. Pavlyukevich, G. E. Gorelik, V. V. Levdanskii', et al., Physical Kinetics and Processes of Heat Transfer in Phase Transformations [in Russian], S. I. Anisimov, (ed.), Minsk (1980).